eprints@whiterose.ac.uk
https://eprints.whiterose.ac.uk/

Comparative Study of Torque Production in Conventional and Mutually Coupled SRMs using Frozen Permeability

G. J. Li, Member, IEEE, Z. Q. Zhu, Fellow, IEEE, X. Y. Ma, and G. W. Jewell

Abstract — This paper investigates the influence of mutual fluxes (inductances) on the resultant torque in 3-phase conventional switched reluctance machine (CSRM) and mutually coupled (MC) SRM using frozen permeability (FP) method. Under saturation conditions, the FP method allows accurately separating the torques due to self and mutual fluxes, and hence quantifying their contributions to torque generation. Then, appropriate current waveforms (unipolar or bipolar, square wave or sinewave) can be established to maximize the output torques. It is well known that the mutual torque of CSRM can be negligible. However, this paper has shown that when sinewave current is employed and under full or overload conditions, the torque will be significantly reduced due to non-negligible negative mutual torques. Different from CSRM, the self and mutual torques of MCSRM can be additive if current waveform is properly chosen, e.g. sinewave currents. This can significantly boost the resultant torque. The predictions have been validated by experiments.

Index Terms — finite element, frozen permeability, mutually coupled SRM, non-linear, self/mutual torque.

I. INTRODUCTION

S WITCHED Reluctance Machines (SRMs), due to their features such as rare earth magnet free and hence low cost, structural simplicity and hence high robustness, etc. are particularly advantageous for safety-critical and harsh environment applications [1]-[3]. For conventional SRMs (CSRMs), square wave, unipolar and non-overlapping phase currents (conduction angle ≤ 120 elec. deg.) are often used due to negligible mutual inductances. This leads to great variation of radial magnetic force acting on the stator over a cycle of rotor rotation. Together with position varying reluctance, the SRMs inherently exhibit higher vibration and acoustic noise when compared to permanent magnet machines [4]-[5].

In order to more efficiently utilise the electric circuit and improve the performance of SRMs, some non-conventional SRMs have been introduced during the last two decades [6]-[7]. In [8]-[10], a fully pitched SRM has been proposed so that the mutual inductances can be fully utilised for torque generation. In these SRMs, the self-inductances are nearly independent of rotor position. As a result, contrary to CSRMs, the torque of fully pitched SRMs is purely produced by the rate of change of mutual inductances with respect to rotor position. However, in order to obtain the torque produced by mutual inductances, the unipolar or bipolar (square wave or sinewave) overlapping phase currents are required. Although it has been proven that for the same copper losses, the fully pitched SRMs can produce higher average torque than conventional short pitched SRMs, their longer end-winding are still problematic. This could restrict their utilisations in volume-sensitive applications such as "more electric" air-craft and electric vehicles.

To overcome the long end-winding issue while still using mutual inductances for torque generation, a new mutually coupled (MC-) SRM has been proposed in [11] and has been extensively studied in [12]-[14]. The MCSRM [see Fig. 1 (b)] has concentrated and short-pitched windings as CSRMs [see Fig. 1 (a)]. This leads to a much shorter end-winding when compared to its fully pitched counterpart. Meanwhile, due to non-negligible mutual inductances, the torque produced by MCSRM could be much higher than that produced by CSRM. This is especially the case when both machines are supplied by sinewave currents. The sinewave current is preferable because a classic converter as that for synchronous machines can be used. Moreover, the vibration and acoustic noises can be mitigated compared to square wave currents [15]. However, when sinewave current is applied, the torque due to mutual inductance of CSRM cannot be neglected anymore, as will be investigated in this paper. Moreover, the contribution of mutual inductance of MCSRM to torque generation will be quantified using the frozen permeability (FP) method. It is worth mentioning that the SRMs supplied by sinewave currents are equivalent to short pitched synchronous reluctance machines (SynRMs). However, for consistency with literature, they will still be called "SRMs" throughout this paper.

It has been identified that the better performance of MCSRM over CSRM is mainly due to two factors, i.e. higher mutual flux (or inductance) and lower magnetic saturation. However, to which extent these two factors will influence the machine performance has not been investigated. In order to fill in this gap, the FP method will be used in this paper so the torque produced by self and mutual fluxes can be separated and then analysed. The FP method accounting for magnetic saturation and cross-coupling is increasingly being used in permanent magnet machines to calculate on-load cogging torque and on-load phase back-EMF, etc. [16]-[19]. However, it has hardly been used in SRMs. This paper will introduce this method to SRMs to accurately separate the torque components produced by self and mutual fluxes of SRMs. As a result, the quantification of torque components due to self and mutual fluxes becomes feasible. Meanwhile, appropriate current waveforms can be established for more efficient utilisation of mutual fluxes, and hence for further boosting torque generation, especially for MCSRM. Therefore, the main contributions of this paper will be: (1) the FP method has been introduced to reveal the real torque generation mechanism of SRMS. Traditionally, for CSRM, it is widely recognized that the mutual torque is negligible and its low overloading capability is due to magnetic saturation. However, this paper proves that this

is not true, because when sinewave current is applied, the mutual torque (produced by mutual inductance) is about half of the self torque (produced by self inductance) and always negative, and hence reduces the total output torque and also leads to low overloading capability. Moreover, for MCSRM, using the FP method, it reveals that both self and mutual torques contribute positively to total output torque, and the mutual torque can be even more significant than the self torque. (2) Since the self and mutual torques can be accurately calculated for both SRMs, the current waveform can be optimized accordingly to achieve higher average torque and/or lower torque ripple.

II. REVIEW OF EXISTING CSRM AND MCSRM

A. Structures of CSRM and MCSRM

The main difference between CSRM and MCSRM exists in their winding arrangements [11]-[14], as shown in Fig. 1. However, the main dimensions of both machines are the same as given in TABLE I for the purpose of comparison.
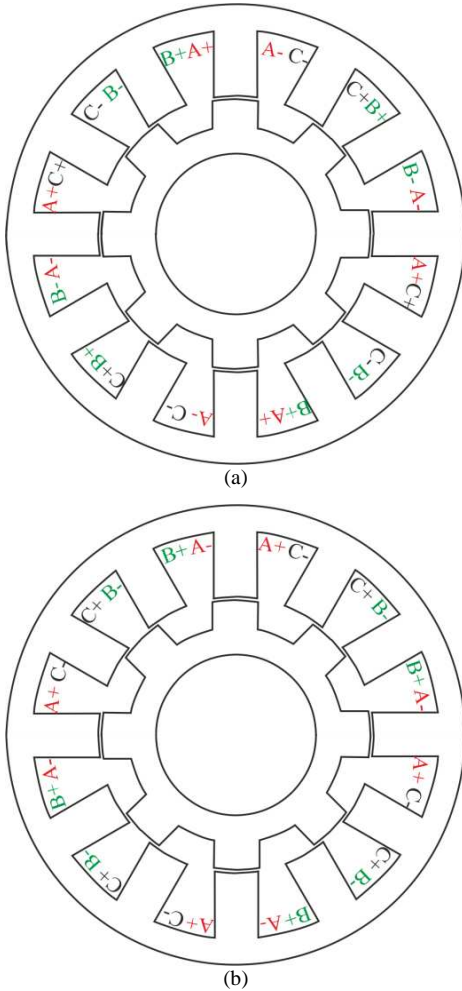

(a)

(b)

Fig. 1 Cross-sectional views of CSRM and MCSRM and their relevant winding arrangements. (a) CSRM, (b) MCSRM.

The CSRM has opposite polarities for any two adjacent coils. This is the same case for the adjacent coils of the same phase (NSNS for coils of phase A). It is worth mentioning that for the investigated 3-phase 12-slot/8-pole double layer CSRM, the

number of coils per phase is 4. Another CSRM with asymmetric coil connection has been investigated in [13], and it is found that although both CSRMs have different winding structures, their electromagnetic performances are similar. Therefore, for simplicity, the CSRM investigated in this paper will only employ the winding structure shown in Fig. 1 (a). However, all coils of MCSRM have the same polarity (NNNN for coils of phase A), as shown in Fig. 1 (b). This difference of coil polarities will have a profound impact on self and mutual flux linkages (inductances), as shown in Fig. 2. As a result, different 3-phase current waveforms, e.g. unipolar square wave (classic), bipolar square wave, or sinewave, can be applied to both CSRM and MCSRM to achieve high average torque. This will be detailed in section III.

TABLE I PARAMETERS OF INVESTIGATED CSRM AND MCSRM

Slot number (N_s)	12	Stator outer radius	45 mm
Pole number (N_r)	8	Stator inner radius	27 mm
Rated current	10 A$_{rms}$	Stack length	60 mm
Torque of CSRM	1.27 Nm	Air-gap length	0.5 mm
Torque of MCSRM	1.43 Nm	Rotor outer radius	26.5 mm

B. Flux plots of CSRM and MCSRM

By way of example, the phase A is supplied by a dc current of 10 A for both SRMs and their flux line distributions are shown in Fig. 2. It is found that for CSRM, at different rotor positions, there are nearly no fluxes produced by phase A crossing through phases B and C. As a result, the mutual fluxes are very low and could be negligible when compared to self fluxes. When it comes to MCSRM, almost half fluxes produced by phase A cross through phase B and the other half cross through phase C for both aligned and unaligned positions. This means that, contrary to CSRM, the mutual fluxes of MCSRM are not negligible for torque production.
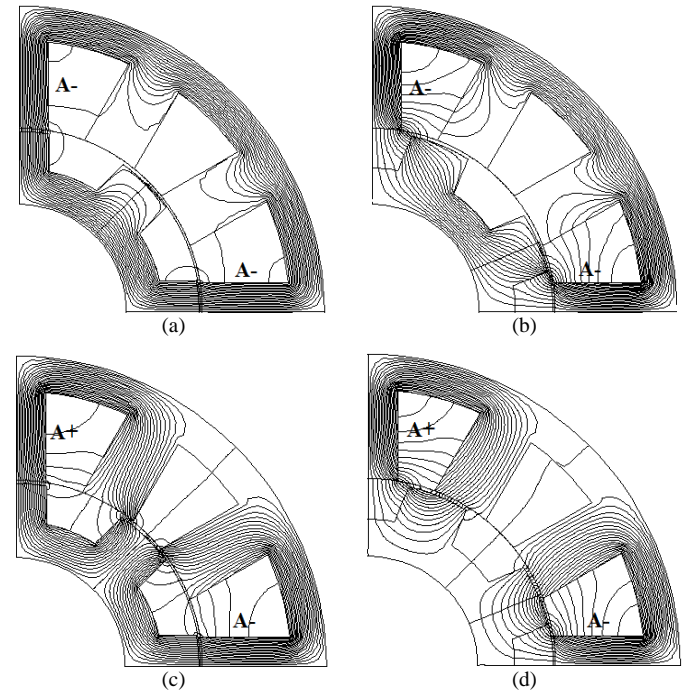

(a)

(b)

(c)

(d)

Fig. 2 Flux plots with phase A supplied by a dc of 10 A. (a) and (b) aligned and unaligned positions of CSRM, (c) and (d) aligned and unaligned positions of MCSRM.

To quantify the self and mutual fluxes of CSRM and MCSRM, they have been calculated for different rotor positions and phase currents by 2-D finite element method (FEM, Opera 2D), as shown in Fig. 3. Again, only the phase A is supplied by dc current. It is well-established that the co-energy (relevant to torque generation) is proportional to the area enveloped by the maximum and minimum flux linkages against phase current. For simplicity, only the maximum and minimum self and mutual flux linkages have been given for both CSRMs and MCSRMs. Based on the co-energy theory, it can be concluded that the torque of MCSRM produced by self flux will be lower than that of CSRM. This is mainly due to the fact that the area enveloped by self flux linkages of MCSRM is only around half of that of CSRM. However, the areas enveloped by self and mutual flux linkages of MCSRM are similar and are substantially larger than the area enveloped by mutual flux linkages of CSRM, which can be negligible. This means that the mutual flux of MCSRM can have significant contribution to torque generation and hence the torque produced by MCSRM could be higher than that of CSRM. Since the polarity of mutual flux can be opposite to that of self flux linkage, their contribution (positive or negative) to torque depends directly on the phase current characteristics (whether the product of two adjacent phase currents is positive or negative). Although it is seen in Fig. 3 that mutual flux exists in MCSRM and will contribute to average torque, when 3-phase are supplied and under overloading conditions, it is impossible to predict how much the contribution of mutual inductance torque is. In this case, the FP method is needed to separate the torques due to self and mutual inductances, respectively, as will be detailed in the following sections.
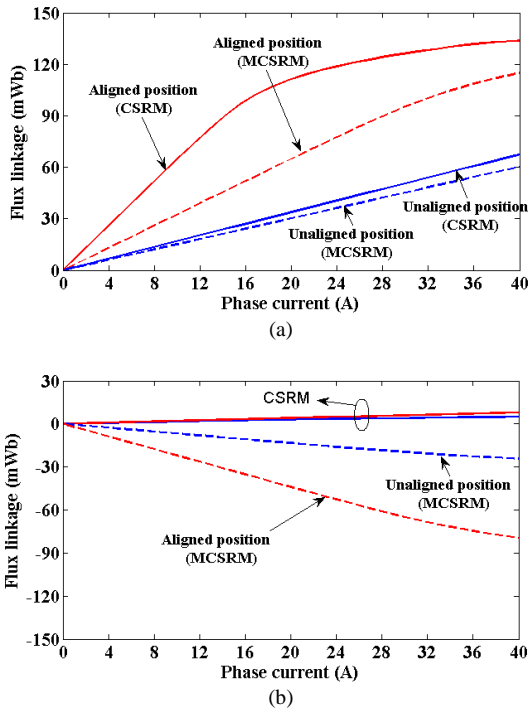

Fig. 3 Self and mutual flux linkages vs phase current for different rotor positions of CSRM and MCSRM. The phase A supplied by dc current and the mutual flux linkage is captured by phase B. (a) self flux linkage, (b) mutual flux linkages.

III. TORQUE SEPARATION USING FROZEN PERMEABILITY FOR SRMS SUPPLIED BY SQUARE WAVE CURRENT

The frozen permeability (FP) method, capable of accounting for magnetic saturation and cross-coupling effects, has been increasingly used in permanent magnet machines to separate fluxes, and torque components produced by armature currents and permanent magnets. Using the FP method, the on-load electromotive force (EMF) and on-load cogging torque, etc. can be accurately calculated [20]-[21]. Similarly, it can also be employed to separate the torque components of SRMs produced by self and mutual inductances under saturated conditions. The implementation procedure of FP method for SRMs is shown in Fig. 2 and summarised in 3 steps as:

(i) Non-linear calculation using static FEM (Vector Field 2D software) is carried out for a given load condition and for different rotor positions. This can give the directly calculated resultant torque or phase flux linkage;

(ii) The relative permeability in all the mesh elements of the FE model for the load conditions in step (i) are then saved and frozen for different rotor positions. This can make sure the magnetic saturation level is unchanged when load condition changes in step (iii);

(iii) Using the same machine geometry (FE model) but with previously saved and frozen permeability in step (ii), the self-flux and torque of each phase can be calculated by resetting the other phase currents to zero. Similarly, the mutual fluxes and torques can also be achieved by subtracting the phase self-fluxes and torques from resultant fluxes and torques [directly calculated by FEM in step (i)], respectively.
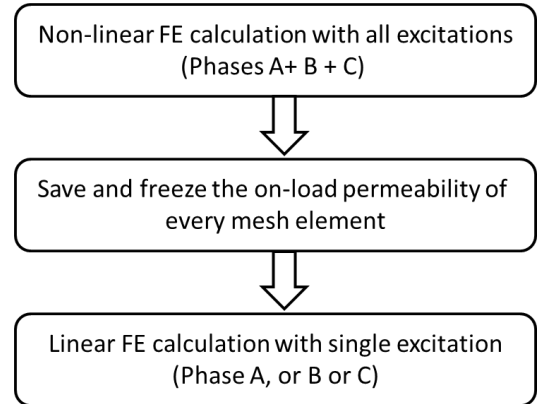

Fig. 4 Implementation procedure of the conventional frozen permeability method for SRMs [19].

A. Validation of Frozen Permeability Method

Before analysing the influence of self and mutual fluxes on the electromagnetic torque of SRMs using the aforementioned FP methods, it is important to validate their accuracy. To this end, both the CSRM and MCSRM are supplied by 3-phase dc currents. A dc current of 40A is used in FE models so to achieve magnetic saturation. Based on the aforementioned principle of FP method, the non-linear calculation has been carried out first [step (i)]. This gives the resultant flux linkage of phase A, i.e. Φ_{A3}, no FP [1 self flux-linkage (Φ_A) + 2 mutual flux-linkages (Φ_{BA} and Φ_{CA})], as shown in Fig. 5, and most importantly the permeability in all the mesh elements of FE model for different rotor positions over one period. Then, the permeability in all the

mesh elements is saved and frozen for further linear calculations [step (ii)].

In order to obtain the on-load self flux-linkage [see Fig. 5, (Φ_{A1}, with FP)], two methods can be applied and then compared:

• First method, a linear 2D FE model with previously saved and frozen permeability in each mesh element has been employed with only the phase A supplied by the same dc current (40 A) [Step (iii)]. As a result, the on-load self flux linkage can be directly calculated.

• Second method, the on-load mutual flux linkages, e.g. Φ_{BA} (between phase A and B), can be calculated when phases A and B are supplied simultaneously by dc currents (40A). This gives a resultant flux linkage of phase A. Subtracting the on-load self-flux linkages of phases A and B can give the on-load mutual flux linkage (Φ_{BA}, with FP). Similarly, the on-load mutual flux linkage between phases A and C (Φ_{CA}, with FP) can be calculated too. For simplicity, only the sum of mutual flux-linkages captured by phase A ($\Phi_{BA} + \Phi_{CA}$, with FP) has been illustrated. As a result, the on-load self flux-linkages can also be calculated using [(Φ_{A3}, no FP) - ($\Phi_{BA} + \Phi_{CA}$, with FP)].

Comparing the on-load self flux-linkages (Φ_{A1}, with FP) and [(Φ_{A3}, no FP) - ($\Phi_{BA} + \Phi_{CA}$, with FP)] obtained by the two aforementioned methods, a perfect match can be observed for both CSRM and MCSRM, and hence proves the accuracy of the FP method used in this paper.
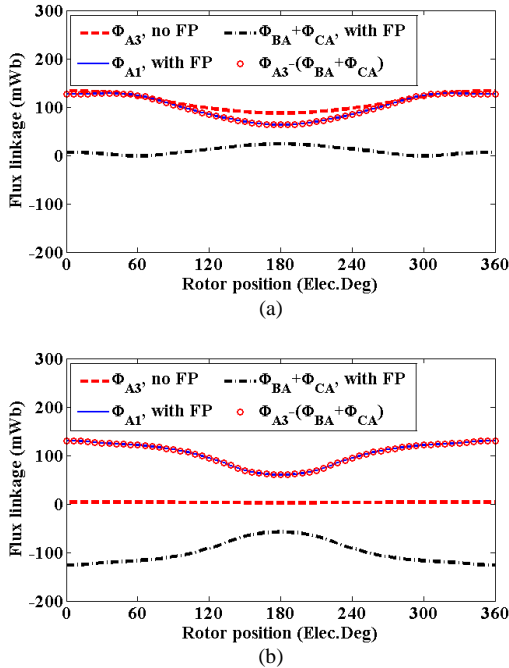

Fig. 5 Flux linkage separation for CSRM and MCSRM supplied by 3-phase dc current using FP method. Phase current is 40A to make sure both machines are heavily saturated. (a) CSRM, (b) MCSRM. Φ_{A1} stands for the self flux of phase A, while Φ_{A3} stands for total flux of phase A (self + mutual fluxes).

B. On-Load Torques of CSRM

The general expression of torque accounting for self and mutual torque components can be expressed by (1). The first three terms on the right hand side of (1) represent the self torques while the last three terms represent the mutual torques.

It is well-established that the equation (1) is only applicable for linear cases. However, with the FP method, self and mutual torques can be accurately calculated even under non-linear conditions. Therefore, the equation (1) will still be applicable for torque analysis even when heavy magnetic saturation occurs.

$$T = \frac{1}{2}\left(\frac{dL_a}{d\theta}I_a^2 + \frac{dL_b}{d\theta}I_b^2 + \frac{dL_c}{d\theta}I_c^2\right) + \left(\frac{dM_{ab}}{d\theta}I_aI_b + \frac{dM_{ac}}{d\theta}I_aI_c + \frac{dM_{bc}}{d\theta}I_bI_c\right) \quad (1)$$

where θ is the rotor position. L_a, L_b, L_c, I_a, I_b and I_c are self-inductances and currents of phases A, B, and C, respectively. M_{ab}, M_{ac}, and M_{bc} are the mutual inductances between phases A, B and C, respectively. The torque ripple coefficient (ΔT) can be calculated by

$$\Delta T(\%) = \frac{T_{max} - T_{min}}{T_{av}} \times 100 \quad (2)$$

where T_{max}, T_{min} and T_{av} are the maximum, minimum and average torques over one electrical period.
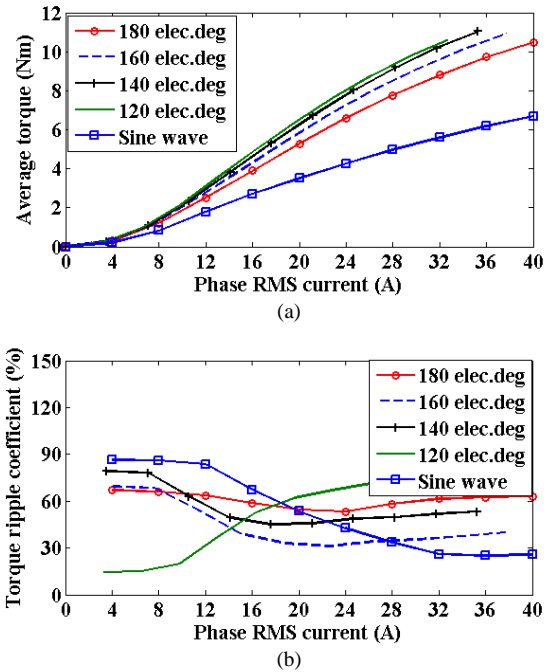

Fig. 6 Average torques and torque ripple coefficients vs phase RMS current and conduction angle of CSRM. All currents are unipolar except the sinewave currents. (a) average torques, (b) torque ripple coefficients.

It is known that for CSRM supplied by 3-phase unipolar and square wave currents, the conduction angle should be 120 elec. deg. [see Fig. 8 (b)] or even smaller to more effectively utilise self-inductance for torque generation. Moreover, the overlapping in unipolar current waveforms could bring in a negative mutual torque, and hence reduce the resultant torque [22]. This is also proven by the results shown in Fig. 6. It is found that the 3-phase unipolar currents with a conduction angle of 120 elec. deg. produces the highest average torque while higher conduction angle leads to lower average torque. As mentioned previously, similar to SynRMs, the CSRM can also be supplied by 3-phase sinewave currents to reduce the vibration and acoustic noises and also to use classic 3-phase converter that has been used for other synchronous machines

and induction machines [15]. However, the sinewave current produces the highest negative mutual torque as can be seen in Fig. 7, and hence results in the lowest resultant torque. This proves that under full or overloading conditions (heavy saturation) the mutual torque cannot be neglected.
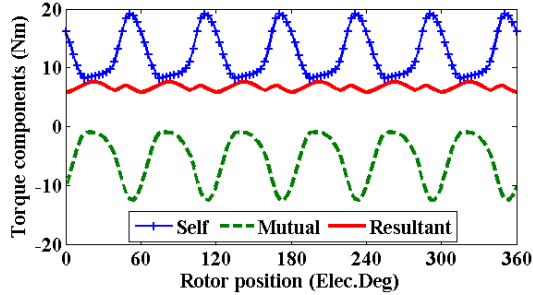

Fig. 7 Torque components of CSRM supplied by sinewave currents with phase RMS current of 40A. Self is the total torque produced by 3-phase self flux linkages, Mutual is the total torque produced by all mutual flux linkages, while Resultant is the sum of Self and Mutual torques. Phase advanced angle is 45 elec.degs., where d- and q-axes currents are equal (SynRMs).

C. On-Load Torques of MCSRM

Due to its different winding structure than CSRM, the MCSRM has negative mutual flux linkages (see Fig. 3) and hence negative mutual inductances. However, if the current waveforms are properly chosen, the mutual inductances can also contribute to positive torque like self-inductances. In order to determine the appropriate current waveforms, the self and mutual torques against rotor position have been calculated using the previously validated FP method, as shown in Fig. 8 (a) and Fig. 9 (a). This is similar to the calculation carried out in Fig. 7 whilst the 3-phase currents are all dc (40A). It is found that the mutual torques have the same periodicity as self torques while with much higher magnitude. This shows the dominance of mutual torque in the torque production of MCSRM.
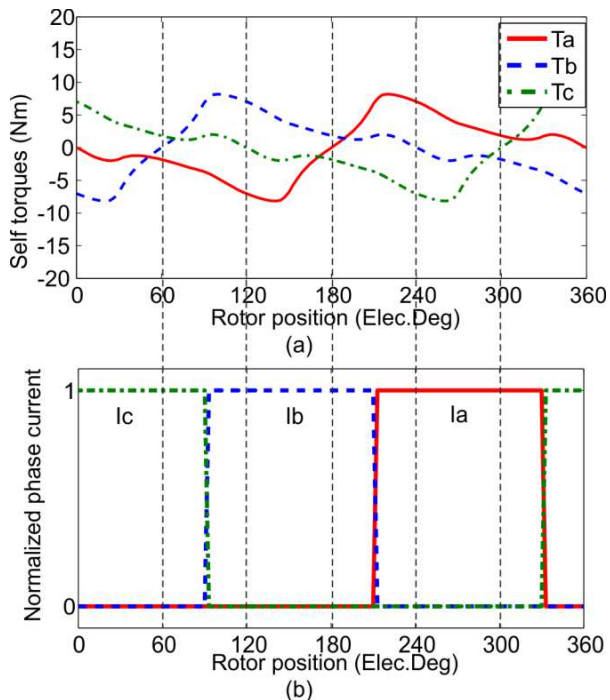

Fig. 8 Self torques and relevant currents for achieving high self torque of MCSRM. The conduction angle is 120 elec. degs. (a) self torques, (b) phase currents.

Based on the obtained self and mutual torques, currents with different waveforms can be chosen to supply the MCSRM. By way of example, the unipolar currents with 120 elec. deg. conduction angle have been employed in Fig. 8 (b) to achieve the highest self torque. However, bipolar currents with 360 elec. deg. conduction angle [see Fig. 9 (b)] can be adopted to achieve the highest mutual torque. As for CSRM, when the conduction angle is 120 elec. deg., there will be no overlap in phase currents and hence no mutual torque. However, the bipolar currents with 360 elec. deg. conduction angle have the highest overlap and hence can achieve the highest positive mutual torque.
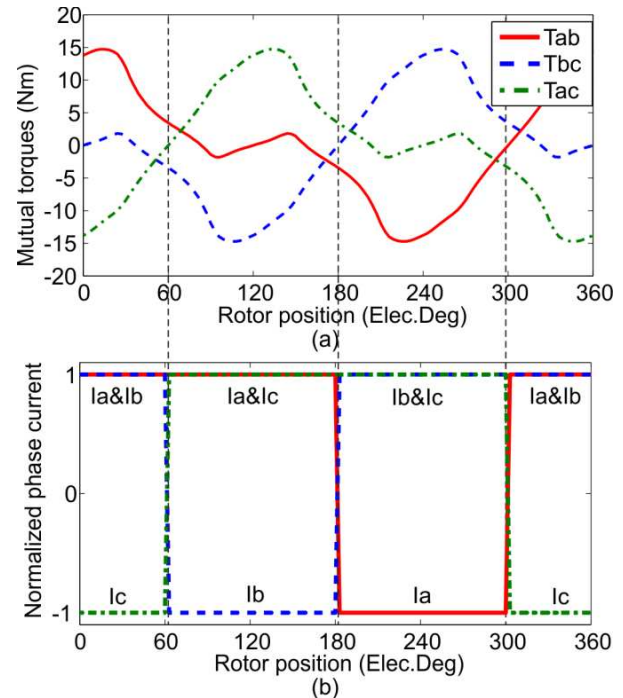

Fig. 9 Mutual torques and relevant currents for achieving high mutual torque of MCSRM. The conduction angle is 360 elec. degs. (120 elec. deg. negative + 240 elec. deg. positive). (a) mutual torques, (b) phase currents.

For further clarity, the choice of current waveforms in Fig. 9 (b) can be explained as follows:
- From 0 to 60 elec. deg., the mutual torque produced by phases B and C (Tbc) is negligible when compared to Tab (>0) and Tac (<0). Therefore, the 3-phase currents should be Ia = Ib = -Ic = I (I is a dc current) so as to have both positive Tab and Tac.
- From 60 to 180 elec. deg., Tab is negligible. To achieve positive Tbc and Tac, the 3-phase currents should be Ia = -Ib = Ic = I.
- Similar approaches can be taken for the rest of the electrical period, giving the current waveforms shown in Fig. 9 (b).

Based on the current waveforms shown in Fig. 9 (b), the torque components of MCSRM have been calculated using the FP method, as shown in Fig. 10. It is found that the total self torque is always negative and its absolute value is only about half of total mutual torque. This is expectable because the current waveforms shown in Fig. 9 (b) are only for achieving high mutual torque without considering the influence on self torque.
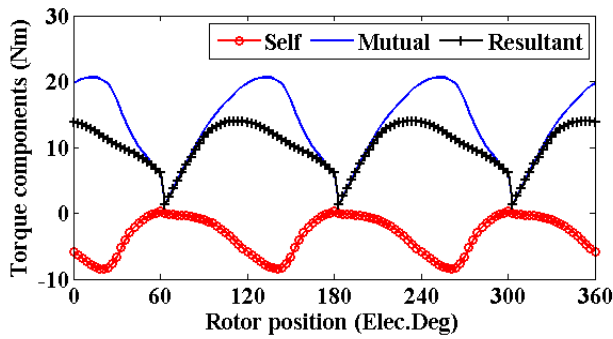
Fig. 10 Torque component separation using FP. The phase RMS current is 40A and the conduction angle is 360 elec. deg. such as shown in Fig. 9 (b).
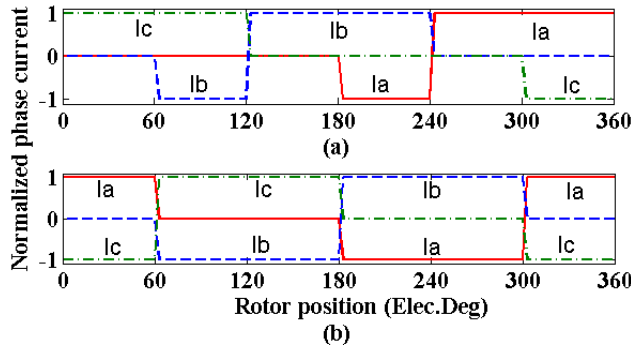

Fig. 11 Square wave currents with different conduction angles. (a) 180 elec. deg. (60 elec. deg. negative + 120 elec. deg. positive), (b) 240 elec. deg. (120 elec. deg. positive + 120 elec. deg. negative).
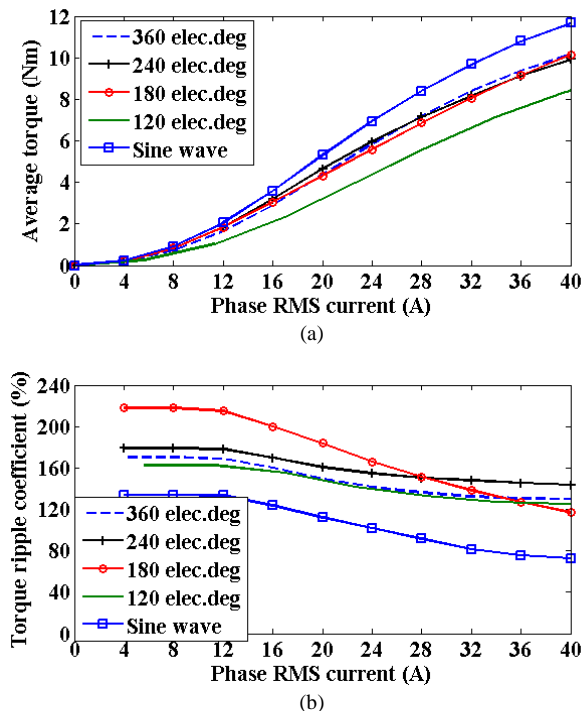

Fig. 12 Average torques and torque ripple coefficients vs phase RMS current and conduction angle of MCSRM. (a) average torques, (b) torque ripple coefficients.

To achieve balanced self and mutual torques and hence to optimise the resultant torque, other bipolar currents with different conduction angles, as shown in Fig. 11, can be used. The average torques and torque ripple coefficients against

phase RMS current have been compared in Fig. 12, in which the results obtained with sinewave currents are added for completeness. It is found that, as long as the mutual torque is involved, the resultant torque can always be improved when compared to the conduction angle of 120 elec. deg. which does not produce mutual torque. The other square wave currents produce similar average torques. However, they are all lower than that produced by sinewave currents, especially at high phase current. In addition, the sinewave currents also have the lowest torque ripple coefficient. It is worth mentioning that the torque ripple can be reduced by shifting the excitation current [23] or shaping the current waveforms [24] or modifying the rotor structure [25], etc. which are out of the main scope of this paper and hence will not be investigated in depth.

D. Torque Comparison for SRMs Supplied by Sinewave Currents

From Fig. 6 and Fig. 12, it is found that when the conduction angle is 120 elec. deg., the CSRM produces much higher average torque than MCSRM, as predicted by Fig. 3 (a). However, with overlapping currents, especially sinewave currents, the MCSRM can produce significantly higher average torque than CSRM. This can be explained by using the results shown in Fig. 13 and Fig. 14, in which both the CSRM and MCSRM are supplied by 3-phase sinewave currents. It can be seen that the self torque of CSRM is always higher than that of MCSRM for the full range of current phase advanced angle and phase RMS current. However, due to non-negligible and negative mutual torque, the resultant torque of the CSRM is much lower than that of the MCSRM that has positive self and mutual torques. In addition, the mutual torque of MCSRM can be much higher than its self torque, especially under overloading conditions. This again shows the dominance of mutual torque for the MCSRM supplied by sinewave currents.
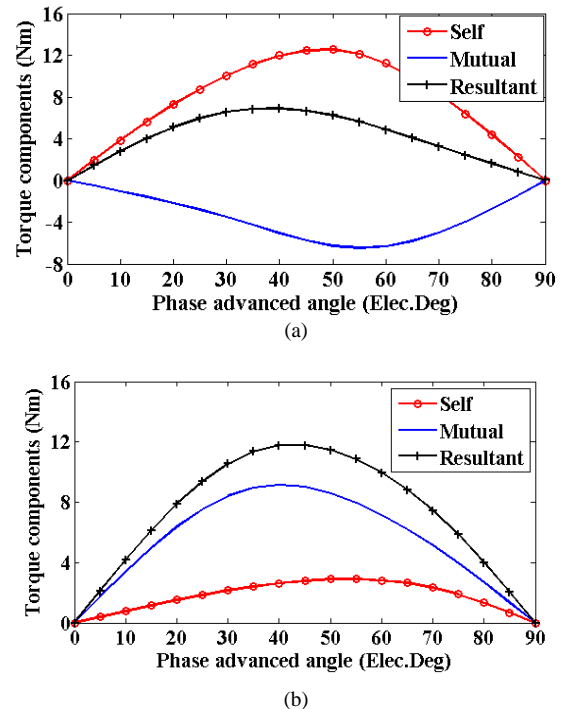

Fig. 13 Self, mutual and resultant torques vs current phase advanced angle. (a) CSRM, (b) MCSRM. Phase RMS current is 40A.
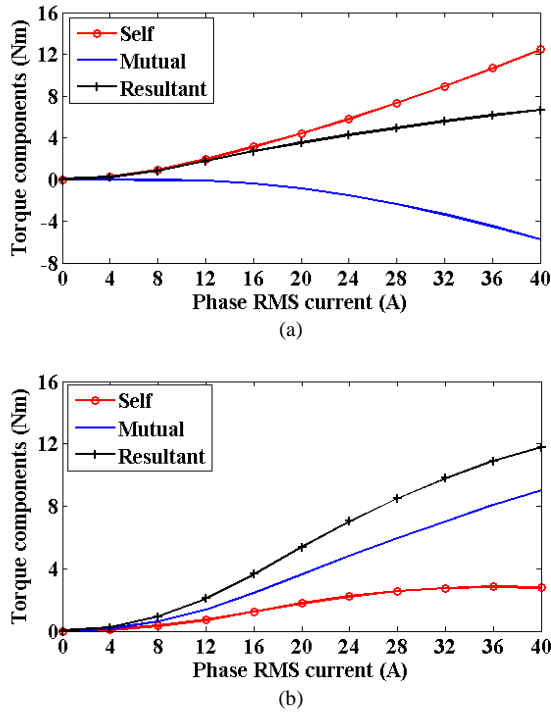
(a)

(b)

Fig. 14 Self, mutual and resultant torques vs phase RMS current. (a) CSRM, (b) MCSRM. Phase advanced angle is 45 elec.degs.

IV. EXPERIMENTAL VALIDATIONS

A. Prototypes of SRMs

In order to validate previously obtained numerical results, a prototype SRM with 12-slot/8-pole has been built, as shown in Fig. 15. The parameters are the same as given in TABLE I. By changing the winding connections, both CSRM and MCSRM topology can be achieved.
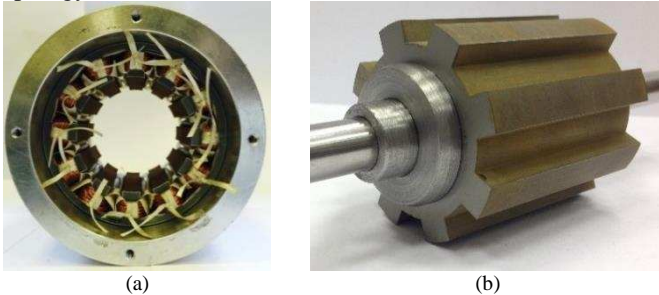

(a)   (b)

Fig. 15 CSRM and MCSRM prototypes. (a) 12-slot stator, (b) 8-pole rotor.
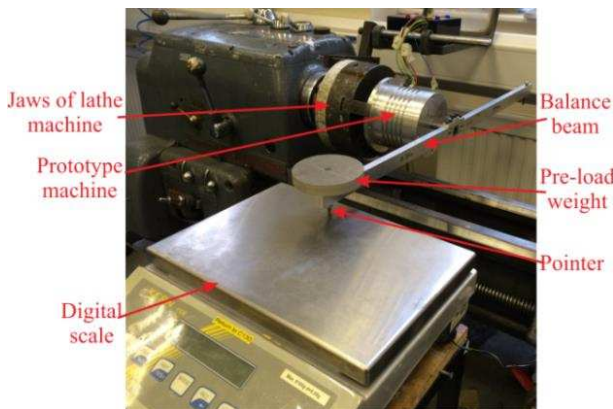

Fig. 16 Test rig for static torque measurements.

B. Torque separation

The static torques can be measured by similar method developed in [26] and the test rig is shown in Fig. 16. A balance beam is connected to the rotor shaft. It is levelled and the bar at one end is rested on the tray of a digital gauge. The stator is clamped in the jaws of a lathe enabling it to be rotated in precise step instead of rotating rotor shaft. By measuring the force [F(N)] using the digital gauge and knowing the distance [l(m)] of the balance beam from shaft center to the pointer, the static torque can be obtained by F(N) × l(m).
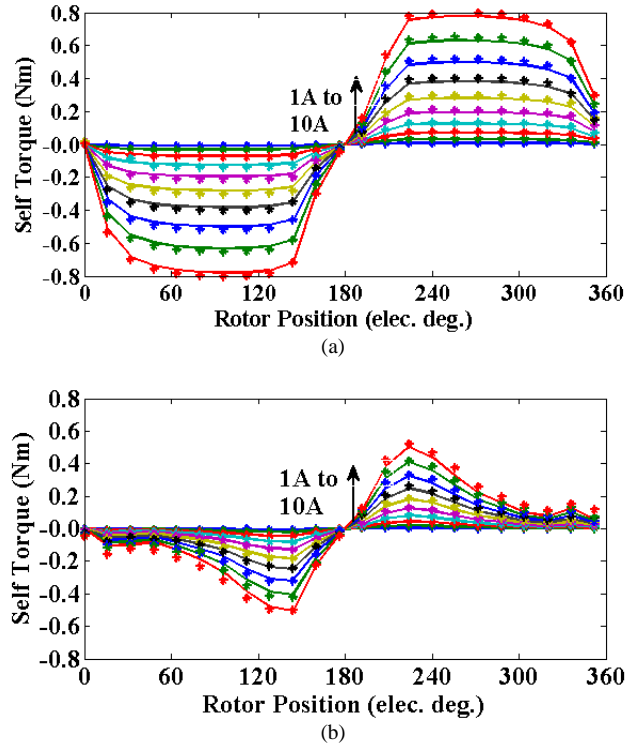

(a)

(b)

Fig. 17 Self torques. (a) self torques of CSRM, (b) self torques of MCSRM. In (a) and (b), solid line: predicted results, dot: measured results.

The self torque can be measured by supplying only one phase (phase A) with a dc current, as shown in Fig. 17. However, to measure the mutual torque and also to validate the FP method for torque separation, the following process needs to be carried out. First, a small dc current (1A) needs to be chosen so to avoid heavy saturation. This is due to the fact that if saturation occurs, it is nearly impossible to accurately separate torque components by experiments, which also proves the necessity of using the FP method for torque components separation. Second, connect two phases in series, e.g. A and B, which will be supplied by this dc current (1A) and the resultant torque can be measured, as shown in Fig. 18 (a) and (b) (Ta + Tb + Tab). Then, supply the two phases independently using the same dc current so two self torques can be measured and the resultant self torque is (Ta + Tb). As a result, the mutual torque is equal to the resultant torque subtracting the resultant self torque, as shown in Fig. 18 (c). A good agreement can be observed between the predicted and measured results. The discrepancy in mutual torques, particularly for CSRM [see Fig. 18 (c)] is mainly due to a measuring error because the value of mutual torque of CSRM is too small to be accurately measured.
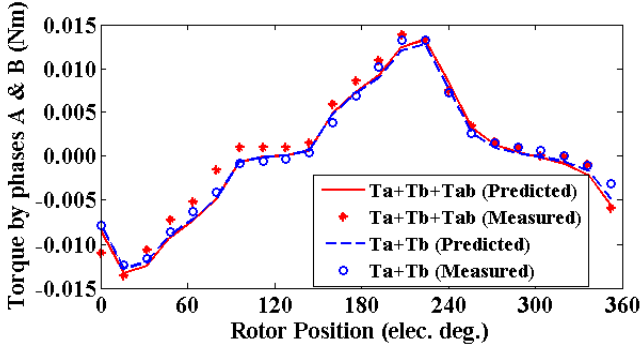
(a)
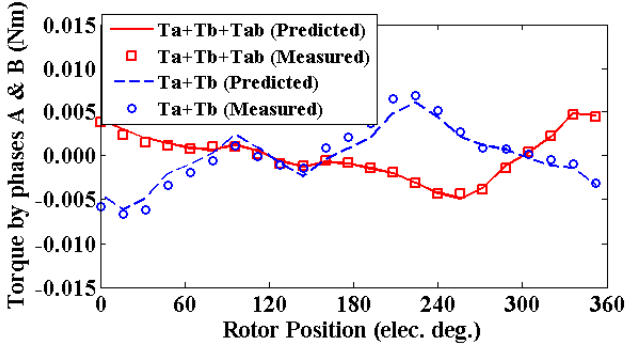
(b)
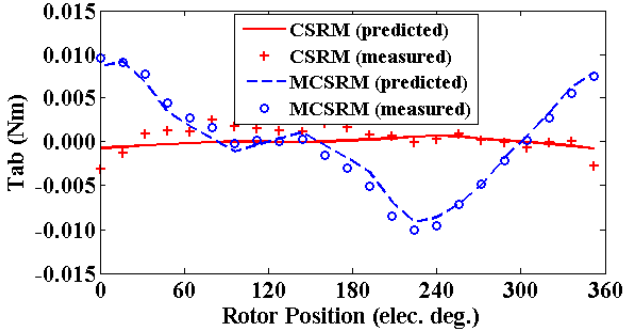
(c)

Fig. 18 Torque components for CSRM and MCSRM with phases A and B supplied by 1 A dc current. (a) resultant torques of CSRM, (b) resultant torques of MCSRM, (c) mutual torques Tab for both SRMs.

C. Static Torque

For the 3-phase tests, the 3 phases of SRMs are supplied by currents such as Ia = I, Ib = -I/2 and Ic = -I/2, where I is dc current which can be varied. As a result, a pseudo-sinewave current condition can be created. It is worth noting that this is only for one rotor position, which is fixed to where the maximum average torque can be achieved. Then, the static torque versus phase RMS current is measured and compared with the predicted results in Fig. 19. The difference between the predicted and measured results mainly comes from the fact that in measurements, the rotor position is difficult to be fixed to be exactly the same as in simulation due to hardware limitations.
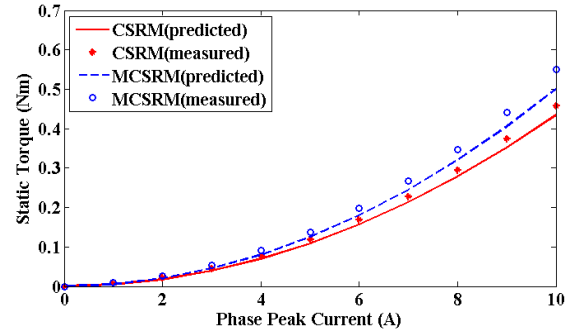

Fig. 19 Predicted and measured static torque vs phase peak current.

V. CONCLUSION

The mutual torque in conventional CSRMs is usually negligible in the previous works due to small mutual flux. However, this paper has found that if overlapping currents are applied, e.g. 3-phase sinewave currents, the mutual torque (negative) can be half of self torque (positive) and reduces significantly the total output torque. Therefore, it cannot be neglected. When it comes to the MCSRMs, the mutual torque (positive) of which can be accurately quantified using the frozen permeability (FP) method and proven to be more significant than self torque (positive) in torque generation. Both SRMs produce relatively high torque ripple, but some techniques such as shifting the excitation current or shaping the current waveforms or modifying the rotor structure may be employed to deal with this problem.

Since the self and mutual torques as functions of rotor position and phase RMS current can be accurately calculated and separated using the FP method, the current waveforms can then be optimised to improve the torque performance of both the CSRM and MCSRM. Experiments have been carried out and the predictions have been validated.

REFERENCES

[1] T. J. E. Miller, "Optimal design of switched reluctance motors," IEEE Trans. Ind. Electron., vol. 49, no. 1, pp. 15-27, Feb. 2002.

[2] W. Ding, L. Liu, J. Y. Lou and Y. P. Liu, "Comparative studies on mutually coupled dual-channel switched reluctance machines with different winding connections," IEEE Trans. Magn., vol. 49, no. 11, pp. 5574-5589, Nov. 2013.

[3] Y. Y. Yang, N. Schofield and A. Emadi, "Double-rotor switched reluctance machine (DRSRM)," IEEE Trans. Energy Conver., vol. 30, no. 2, pp. 671-680, June 2015.

[4] V. P. Vujičić, "Minimization of torque ripple and copper losses in switched reluctance drive," IEEE Trans. Power Electron., vol. 27, no. 1, pp. 388-399, Jan. 2012.

[5] M. Takiguchi, H. Sugimoto, N. Kurihara and A. Chiba, "Acoustic noise and vibration reduction of SRM by elimination of third harmonic component in sum of radial forces," IEEE Trans. Energy Conver., vol. 30, no. 3, pp. 883-891, Sept. 2015.

[6] W. Ding, Y. Hu and L. Wu, "Analysis and development of novel three-phase hybrid magnetic paths switched reluctance motors using modular and segmental structures for EV applications," IEEE/ASME Trans. Mechatron., vol. 20, no. 5, pp. 2437-2451, Oct. 2015.

[7] W. Wang, M. Y. Luo, E. Cosoroaba, B. Fahimi and M. Kiani, "Rotor shape investigation and optimization of double stator switched reluctance machine," IEEE Trans. Magn., vol. 51, no. 3, pp. 1-4, Mar. 2015.

[8] B. C. Mecrow, "Fully pitched-winding switched-reluctance and stepping-motor arrangements," IEE Proc. Elec. Power Appl., vol. 140, no. 1, pp. 61-70, Jan. 1993.

[9] Y. Xu and D. A. Torrey, "Study of the mutually coupled switched reluctance machine using the finite element-circuit coupled method,"

IEE Proc. Elec. Power Appl., vol. 149, no. 2, pp. 81-86, Mar. 2002.

[10] J. D. Widmer and B. C. Mecrow, "Optimized segmental rotor switched reluctance machines with a greater number of rotor segments than stator slots," IEEE Trans. Ind. Appl., vol. 49, no. 4, pp. 1491-1498, July-Aug. 2013.

[11] J. W. Ahn, S. G. Oh, J. W. Moon and Y. M. Hwang, "A three-phase switched reluctance motor with two-phase excitation," IEEE Trans. Ind. Appl., vol. 35, no. 5, pp. 1067-1075, Sep./Oct. 1999.

[12] G. J. Li, J. Ojeda, E. Hoang, M. Lecrivain and M. Gabsi, "Comparative studies between classical and mutually coupled switched reluctance motors using thermal-electromagnetic analysis for driving cycles," IEEE Trans. Magn., vol. 47, no. 4, pp. 839-847, Apr. 2011.

[13] Z. Azar and Z. Q. Zhu, "Investigation of electromagnetic performance of salient-pole synchronous reluctance machines having different concentrated winding connections," in 2013 IEEE Int. Elec. Machines & Drives Conf. (IEMDC), Chicaco, USA, 12-15 May 2013.

[14] X. B. Liang, G. J. Li, J. Ojeda, M. Gabsi and Z. X. Ren, "Comparative study of classical and mutually coupled switched reluctance motors using multiphysics finite-element modeling," IEEE Trans. Ind. Electron., vol. 61, no. 9, pp. 5066-5074, Sept. 2014.

[15] X. Ojeda, X. Mininger, M. Gabsi and M. Lecrivain, "Sinusoidal feeding for switched reluctance machine: application to vibration damping," in ICEM 2008, 6-9 Sept. 2008.

[16] N. Bianchi and S. Bolognani, "Magnetic models of saturated interior permanent magnet motors based on finite element analysis," in Proc. IEEE Ind. Appl. Conf., St. Louis, MO, USA, 12-15 Oct. 1998.

[17] D. M. Ionel, M. Popescu, M. I. McGilp, T. J. E. Miller and S. J. Dellinger, "Assessment of torque components in brushless permanent-magnet machines through numerical analysis of the electromagnetic field," IEEE Trans. Ind. Appl., vol. 41, no. 5, pp. 1149-1158, Sept.-Oct. 2005.

[18] Z. Azar, Z. Q. Zhu and G. Ombach, "Influence of electric loading and magnetic saturation on cogging torque, back-EMF and torque ripple of PM machines," IEEE Trans. Magn., vol. 48, no. 10, pp. 2650-2658, Oct. 2012.

[19] W. Q. Chu and Z. Q. Zhu, "Average torque separation in permanent magnet synchronous machines using frozen permeability," IEEE Trans. Magn., vol. 49, no. 3, pp. 1202-1210, Mar. 2013.

[20] J. A. Walker, D. G. Dorrell and C. Cossar, "Flux-linkage calculation in permanent-magnet motors using the frozen permeabilities method," IEEE Trans. Magn., vol. 41, no. 10, pp. 3946-3948, Oct. 2005.

[21] W. Q. Chu and Z. Q. Zhu, "On-load cogging torque calculation in permanent magnet machines," IEEE Trans. Magn., vol. 49, no. 6, pp. 2982-2989, June 2013.

[22] J. A. Walker, D. G. Dorrell and C. Cossar, "Effect of mutual coupling on torque production in switched reluctance motors," Journal of Applied Physics, vol. 99, no. 8, pp. 08R304-3, Apr. 2006.

[23] V. Nasirian, A. Davoudi, S. Kaboli and C. S. Edrington, "Excitation shifting: a general low-cost solution for eliminating ultra-low-frequency torque ripple in switched reluctance machines," IEEE Trans. Magn., vol. 49, no. 9, pp. 5135-5149, Sept. 2013.

[24] R. Mikail, I. Husain, M. S. Islam, Y. Sozer and T. Sebastian, "Four-quadrant torque ripple minimization of switched reluctance machine through current profiling with mitigation of rotor eccentricity problem and sensor errors," IEEE Trans. Ind. Appl., vol. 51, no. 3, pp. 2097-2104, May-June 2015.

[25] G. J. Li, J. Ojeda, S. Hlioui, E. Hoang, M. Lecrivain and M. Gabsi, "Modification in rotor pole geometry of mutually coupled switched reluctance machine for torque ripple mitigating," IEEE Trans. Magn., vol. 48, no. 6, pp. 2025-2034, June 2012.

[26] Z. Q. Zhu, "A simple method for measuring cogging torque in permanent magnet machines," in IEEE Power & Energy Society General Meeting, 26-30 Jul. 2009.